Radiation-induced alloy rearrangement in $In_xGa_{1-x}N$

V. Prozheeva, I. Makkonen, R. Cuscó, L. Artús, A. Dadgar, F. Plazaola, and F. Tuomisto

Citation: Appl. Phys. Lett. **110**, 132104 (2017); doi: 10.1063/1.4979410

View online: http://dx.doi.org/10.1063/1.4979410

View Table of Contents: http://aip.scitation.org/toc/apl/110/13

Published by the American Institute of Physics

Radiation-induced alloy rearrangement in $In_xGa_{1-x}N$

V. Prozheeva,[1] I. Makkonen,[1] R. Cuscó,[2] L. Artús,[2] A. Dadgar,[3] F. Plazaola,[4] and F. Tuomisto[1]

[1]*Department of Applied Physics, Aalto University School of Science, P.O. Box 15100, FI-00076 Aalto, Finland*
[2]*Institut Jaume Almera (ICTJA-CSIC), Consejo Superior de Investigaciones Cientificas, 08028 Barcelona, Spain*
[3]*Institut für Experimentelle Physik, Otto-von-Guericke-Universität Magdeburg, 39016 Magdeburg, Germany*
[4]*Elektrizitatea eta Elektronika Saila, UPV-EHU, P.K. 644, 48080 Bilbao, Spain*

(Received 17 January 2017; accepted 11 March 2017; published online 30 March 2017)

The effect of radiation damage on the defect and alloy structure in $In_xGa_{1-x}N$ thin films grown on Si substrates was studied using positron annihilation spectroscopy. Prior to the measurements, the samples were subjected to double He^+ implantation at 40 and 100 keV. The results show the presence of cation vacancy-like defects in high concentrations ($>10^{18}\,cm^{-3}$) already in the as-grown samples. The evolution of the annihilation characteristics after the implantation suggests strong alloy disorder rearrangement under irradiation. *Published by AIP Publishing.* [http://dx.doi.org/10.1063/1.4979410]

Following the breakthrough in manufacturing of efficient blue light-emitting diodes (LEDs), devices operating in the wavelength range 500–570 nm need to be optimized next. The most promising candidate for building a path across the green LED field is expected to be $In_xGa_{1-x}N$. Alloying GaN with InN enables the development of a platform with combined blue and green LEDs based on a homogeneous system. However, the required indium content of at least 25% in alloys[1] leads to defect formation[2] and subsequent deterioration of electrical properties and decrease of device efficiency. On the other hand, the adjustable direct band gap and exceptional resistance to irradiation damage enable the application of $In_xGa_{1-x}N$ in solar cells for outer space.[3–5] Further integration with silicon promises even more: the band alignment at the $In_xGa_{1-x}N$/Si heterointerface eliminates the need for heavy doping, and the energy conversion efficiencies were shown to reach 31% and 35% for two- and three-junction $In_xGa_{1-x}N$/Si solar cells, respectively.[6,7] Despite the lattice mismatch with Si and induced cracking and high dislocation density, several successful attempts to grow $In_xGa_{1-x}N$/Si-based structures have been declared.[8–10]

Leaving the expectations aside, surprisingly little is known about defect structure in $In_xGa_{1-x}N$ alloys. So far, inhomogeneous indium distribution, dislocations, and surface-related defects have been reported.[11–14] Cation vacancies have been predicted to play a crucial role in Shockley-Read-Hall recombination in wide-band-gap semiconductors.[15] Experimental studies of vacancy-type defects in thin-film III-nitrides have been extensively performed by positron annihilation spectroscopy (see Refs. 16–18 and references therein). The sensitivity of positrons is not affected by conductivity of samples,[19] making them especially suitable for studying $In_xGa_{1-x}N$-based structures.

In this work, we apply positron annihilation spectroscopy to study the effect of radiation damage on the defect and alloy structure in $In_xGa_{1-x}N$ thin films. The as-grown samples films contain cation vacancies with concentrations in the $10^{18}\,cm^{-3}$ range with characteristics reflecting the random site distribution of In and Ga atoms in the lattice. Upon He^+ implantation, the nature of the introduced cation vacancy defects gradually changes with increasing fluence towards that of the indium vacancy V_{In} in InN, reflecting a change in the distribution of the metal atoms and indicating the generation of indium-rich regions in the lattice.

The $In_xGa_{1-x}N$ samples were grown by metal-organic chemical vapour deposition on 10-nm-thick $In_xAl_{1-x}N$ buffer layers deposited on Si (111) substrates. The thicknesses of the samples with $x = 0.37$ and $x = 0.45$ are 463 nm and 446 nm, respectively. Samples 3 and 4 were superficially etched with nitric acid. The samples were doubly implanted at energies of 40 keV and 100 keV with He^+ fluences calculated to obtain a homogeneous damage profile over the whole layer thickness. Each pair of He^+ implantation fluences for the respective samples ranging from $10^{12}\,cm^{-2}$ to $10^{15}\,cm^{-2}$ is listed in Table I. The implantation-induced damage was estimated with Stopping and Range of Ions in Matter (SRIM) code.[20] He^+ implantation with a similar fluence and damage level has been shown to produce single cation vacancy-type defects in InN.[21]

Positron annihilation spectroscopy is an efficient method for identification of negatively charged and neutral vacancy-type defects.[19] The momentum of the positron-electron pair is conserved in the annihilation event. The momentum distribution corresponds to the measured Doppler broadening of the annihilation photons. The shape of the Doppler broadened annihilation line (often characterized by the conventional S and W parameters) gives detailed information about the identity and concentration of the vacancy-type defects present. The S (W) parameter reflects the annihilations with valence (core) electrons and is defined as a fraction of counts in the central region (wing areas) of the Doppler peak. The decreased electron density on a vacancy cite is typically reflected as an increase of positron lifetime and the narrowing of the 511 keV photo-peak in the annihilation gamma spectrum, compared to a defect-free crystal. In this work, the Doppler broadening spectra were measured using a monoenergetic positron beam at room temperature. The measurements were performed with a high purity germanium detector, with an energy resolution of 1.3 keV at 511 keV. Each set of measurements consists of a series of

TABLE I. Growth parameters and properties of $In_xGa_{1-x}N$ thin film samples. Samples 3 and 4 are as-grown samples chemically etched with HNO_3. Displacement damage dose parameter D_d is defined as the product of the non-ionizing energy loss and the particle fluence. For the implanted samples, the implantation-induced damage was estimated with SRIM code. The vacancy concentration in the non-implanted samples was estimated from positron annihilation experiments.

			He^+ fluence			
Sample	d, nm	x	at 40 keV (cm^{-2})	at 100 keV (cm^{-2})	D_d (MeV/g)	Vacancy concentration (cm^{-3})
1/2	463/446	0.37/0.45	…	…	…	$>10^{18}$
3/4	463/446	0.37/0.45	…	…	…	$>10^{18}$
A/B	463/446	0.37/0.45	1.4×10^{12}	3.7×10^{12}	8.0×10^{13}	9×10^{18}
C/D	463/446	0.37/0.45	8.9×10^{12}	2.3×10^{13}	5.0×10^{14}	6×10^{19}
E/F	463/446	0.37/0.45	5.7×10^{13}	1.5×10^{14}	3.2×10^{15}	3×10^{20}
G/H	463/446	0.37/0.45	3.6×10^{14}	9.3×10^{14}	2.0×10^{16}	2×10^{21}

spectra with approximately 1×10^6 counts recorded as a function of positron implantation energy in the range 0.5–35 keV.

The electronic structure calculations for bulk systems were performed using a 16-atom $In_xGa_{1-x}N$ wurtzite supercell. For systems containing a vacancy, the supercell size was increased to 128 atoms. The structures were modelled using the local-density approximation (LDA) for exchange and correlation[22] as implemented in the VASP code.[23,24] Positron states are modeled assuming that the positron does not affect the average electron density and taking the zero-positron limit of the LDA correlation energy and enhancement factor.[25] For localized positrons, we take into account the repulsive forces on ions due to the localized positron. Momentum densities of annihilating electron-positron pairs are calculated using the projector augmented-wave (PAW) method.[24,26]

The results of conventional Doppler measurements for selected samples are presented in Figure 1. The expected

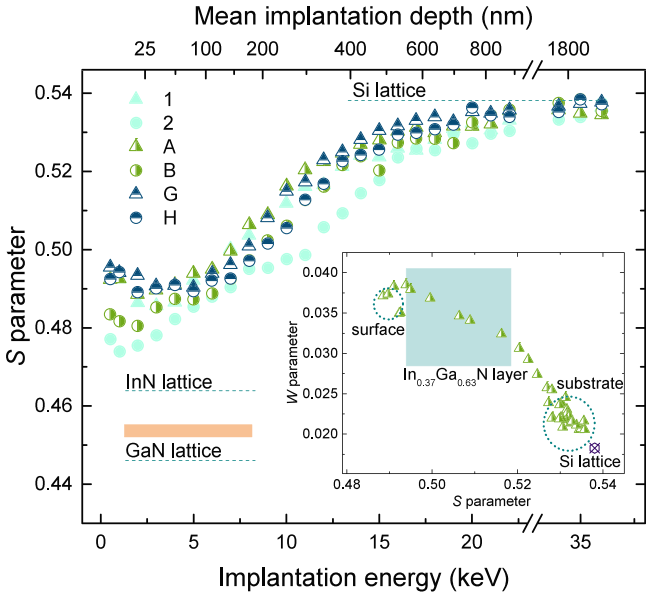

FIG. 1. The S parameter as a function of positron implantation energy and mean implantation depth in as-grown, the lowest and the highest fluence He^+-implanted samples. The highlighted region between the InN and GaN lattice S values depicts the S parameter for defect-free $In_xGa_{1-x}N$ with $0.37 < x < 0.5$ (Ref. 28). The skipped data in the range from 23 to 33 keV are consistent with the presented values at high implantation energies. Inset: the (S, W) plot for sample A. The surface, layer, and substrate regions are marked. The data at the far extent of the $In_xGa_{1-x}N$ layer are not yet affected by the Si substrate.

values for defect-free $In_xGa_{1-x}N$ with 37% and 45% In are found between the characteristic (S, W) parameters for the InN and GaN lattices.[16,27] The reference (S, W) parameters (for GaN $S_{ref} = 0.44(6)$ and $W_{ref} = 0.054(4)$) are obtained from samples where positrons annihilate in the delocalized state in the lattice. The slightly higher values of the S parameter in the samples at low energies result from annihilations at the surface states. When the implantation energy E reaches approximately 4 keV (corresponding mean implantation depth $\simeq$ 60 nm), the dominant fraction of positrons annihilates inside the $In_xGa_{1-x}N$ film. At 15 keV and higher energies, the positrons reach the substrate, thus, the high values of the S parameter are attributed to the annihilations in the Si lattice. The inset in Figure 1 demonstrates the signal obtained from the positrons annihilating from the surface states, in the $In_{0.37}Ga_{0.63}N$ layer and in the Si substrate for sample A in terms of the (S, W) plane. At implantation energies above 10 keV (bottom right corner of the highlighted area), the slope of the layer-related data changes, and the measured values tend towards the (S, W) point characteristic of the Si lattice. The S parameter in all the samples is higher than the characteristic values for the GaN and InN lattices. This, together with the relatively short effective positron diffusion length (no back-diffusion to the surface observed above $E = 4$ keV), indicates that positrons annihilate as trapped at vacancy-type defects in the $In_xGa_{1-x}N$ films.

For a more detailed analysis, we consider the (S, W) plot shown in Figure 2, where the measured parameters are normalized to those obtained in GaN reference sample. Only the data points corresponding to the $In_xGa_{1-x}N$ layer and to the near-interface region between the layer and the substrate are presented (smaller and larger markers, correspondingly). The data between each pair of the depicted (S, W) points follow a linear trend and are thus omitted for clarity. The (S, W) points for GaN and InN lattices are shown for comparison. The dashed-dotted line connecting the GaN and InN extremes represents the (S, W) parameters for defect-free $In_xGa_{1-x}N$ as a function of indium content as shown in Ref. 28. The region in the (S, W) plane corresponding to defect-free alloys with $37\% < x < 50\%$ indium is highlighted. Further, three more anchor points, gallium vacancy V_{Ga} in GaN, and indium vacancy V_{In} and indium vacancy decorated with several nitrogen vacancies V_{In}–nV_N, $n \geq 2$, both in InN, are obtained by combining experiments and theoretical calculations.[16,27,29] The shaded region between V_{Ga} and V_{In} reflects the scatter of

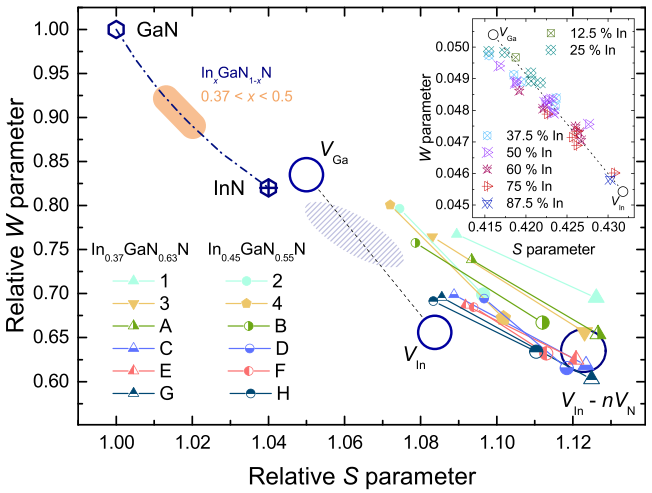

FIG. 2. The (*S*, *W*) values at 4/5 keV (smaller markers) and 9/10 keV (larger markers) normalized to the GaN reference. The dashed-dotted line represents the (*S*, *W*) scattering for defect-free $In_xGa_{1-x}N$. The highlighted region on the GaN–InN line corresponds to defect-free alloys with 37%–50% indium. The shaded region of the V_{Ga}–V_{In} line shows scattering span of the (*S*, *W*) parameters in cation vacancy-containing $In_xGa_{1-x}N$ corresponding to the values presented in the inset. Inset: the calculated *S* and *W* parameters for $In_xGa_{1-x}N$ systems containing a metal vacancy with varying In/Ga distribution as a function of indium content.

the Doppler parameters in $In_xGa_{1-x}N$ systems containing a metal vacancy.[28] The (*S*, *W*) parameters for the InN lattice, V_{In} and V_{In}–nV_N have been as well normalized to the GaN reference. The inset shows the *S* and *W* parameters calculated in $In_xGa_{1-x}N$ systems containing one metal vacancy with different In contents and varying In/Ga distributions.[28] Please note that the calculation results are provided for illustration and cannot be directly compared to the measurement results. Isolated nitrogen vacancies do not trap positrons due to their small size and positive charge state but strongly modify the cation vacancy signal when cation vacancy–nitrogen vacancy complexes are formed.[16,29]

In the as-grown samples 1–4, the layer (*S*, *W*) values lie rather close to one of the extremes of the cation vacancy in $In_xGa_{1-x}N$ systems (the shaded region in Figure 2). In addition, the very short diffusion length seen in Figure 1 implies saturation trapping at group III cation vacancies or vacancy-related complexes, indicating cation vacancy concentration of the order of 10^{18} cm^{-3} or higher. The right shift of data points for samples 1–4 obtained at higher implantation energies in the (*S*, *W*) plane displayed in Figure 2 (larger symbols) can be attributed to cation vacancies complexed with nitrogen vacancies. A similar rightward shift was observed in MBE-grown $In_xGa_{1-x}N$ for V_{III}–mV_N and in InN for V_{In}–nV_N complexes.[16,17] In fact, these $In_xGa_{1-x}N$/Si interface values are very close to those of V_{In}–nV_N calculated for InN indicating an increase in the number of V_N associated with a cation vacancy as shown in Ref. 16 and suggesting higher indium content in the near-interface region. It is unlikely that this observation would reflect preferential formation of cation vacancy defects in the regions of higher indium content in random alloys: the cation vacancy formation energy is higher in InN than in GaN.[30–32]

Considering the $In_xGa_{1-x}N$ layers, after the lowest implantation dose, the data resemble those of the as-grown samples, in line with the estimated concentrations of pre-existing vacancy defects and the SRIM estimate of implantation-induced damage. As the He^+ implantation fluence increases, the nature of the vacancy-type defects in $In_xGa_{1-x}N$ layers clearly changes. For the highest He^+ fluence, the data points in the layers essentially converge towards the V_{In} characteristic value. Hence, either the vacancy defects are mostly created in In-rich regions or formation of In-rich regions is enhanced by high-fluence implantation, leading to increasing positron trapping at vacancies in those regions. Interestingly, despite the increasing implantation dose there is no observable change near the $In_xGa_{1-x}N$/Si interface where the cation vacancies already exhibit V_{In}–nV_N -like character. It should be noted that in III-nitride alloys, the cation shell has the most impact on the positron data, while the lattice parameters play a minor role. In addition, indium vacancy formation in InN under irradiation has been shown to be much less efficient than the formation of gallium vacancies in GaN (Ref. 33) and irradiation damage has been shown to be more important in Ga-rich than in In-rich $In_xGa_{1-x}N$ (Ref. 3). Thus, as there is no reason for enhanced positron annihilation in the regions with higher indium composition naturally occurring in a random distribution, we interpret that either the indium content of the In-rich regions increases or the distribution of the In-rich regions densifies in the implantation by a mechanism mediated by cation vacancies. Similar observations have been made in proton-irradiated $Si_{1-x}Ge_x$: the originally random Si/Ge distribution has changed significantly after introducing vacancy defects by irradiation and then removing them by annealing.[34]

Our interpretation that the In/Ga distribution is modified by radiation damage has important consequences, as the regions with high indium content potentially localize holes efficiently.[35,36] Our findings should not be interpreted as an evidence of indium clusters, the existence of which is a matter of debate.[37,38] Actually, already the random In/Ga composition fluctuations can be enough for hole localization.[39] Intensification of these composition fluctuations as observed in our experiments is likely to lead to stronger hole localization.

In summary, we have applied positron annihilation spectroscopy to investigate the effect of He^+ implantation on the vacancy-type defects in high In-content $In_xGa_{1-x}N$ thin films grown on Si substrates. The annihilation characteristics of the cation vacancy defects detected in the as-grown layers were found to be in agreement with those predicted for random alloys. Closer to the film-substrate interface, the nature of the defects strongly reminds V_{In}–V_N complexes in InN, while heavy radiation damage in the $In_xGa_{1-x}N$ layers leads to annihilation characteristics similar to V_{In} in InN. This points towards the existence of indium-rich regions close to the interface already in as-grown samples and the region expansion after heavy implantation. The latter suggests strong alloy disorder rearrangement under irradiation, an effect that needs to be taken into account when developing $In_xGa_{1-x}N$-based photovoltaic and optoelectronic devices for environments with elevated background radiation.

We acknowledge the computational resources provided by the Aalto Science-IT project. V.P. and I.M. acknowledge financial support from the Academy of Finland (Project Nos.

285809 and 293932). This work has been partially supported by the Spanish MINECO under Contract No. MAT2015-71035-R.

[1]M. A. der Maur, K. Lorenz, and A. D. Carlo, Opt. Quantum Electron. **44**, 83 (2012).
[2]X. Niu, G. B. Stringfellow, and F. Liu, Appl. Phys. Lett. **99**, 213102 (2011).
[3]J. Wu, W. Walukiewicz, K. M. Yu, W. Shan, J. W. Ager, E. E. Haller, H. Lu, W. J. Schaff, W. K. Metzger, and S. Kurtz, J. Appl. Phys. **94**, 6477 (2003).
[4]R. M. Farrell, C. J. Neufeld, S. C. Cruz, J. R. Lang, M. Iza, S. Keller, S. Nakamura, S. P. DenBaars, U. K. Mishra, and J. S. Speck, Appl. Phys. Lett. **98**, 201107 (2011).
[5]C. J. Neufeld, N. G. Toledo, S. C. Cruz, M. Iza, S. P. DenBaars, and U. K. Mishra, Appl. Phys. Lett. **93**, 143502 (2008).
[6]L. Hsu and W. Walukiewicz, J. Appl. Phys. **104**, 024507 (2008).
[7]I. Gherasoiu, L. A. Reichertz, K. M. Yu, J. W. Ager, V. M. Kao, and W. Walukiewicz, Phys. Status Solidi C **8**, 2466 (2011).
[8]P. Kumar, P. E. D. S. Rodriguez, V. J. Gómez, N. H. Alvi, E. Calleja, and R. Nötzel, Appl. Phys. Lett. **6**, 035501 (2013).
[9]F. Reiher, A. Dadgar, J. Bläsing, M. Wieneke, M. Müller, A. Franke, L. Reißmann, J. Christen, and A. Krost, J. Phys. D: Appl. Phys. **42**, 055107 (2009).
[10]L. A. Reichertz, I. Gherasoiu, K. M. Yu, V. M. Kao, W. Walukiewicz, and J. W. Ager III, Appl. Phys. Express **2**, 122202 (2009).
[11]A. Yankovich, A. Kvit, X. Li, F. Zhang, V. Avrutin, H. Liu, N. Izyumska, U. Özgür, H. Morkoc, and P. Voyles, Proc. SPIE **7939**, 79391E (2011).
[12]D. Van Den Broeck, D. Bharrat, Z. Liu, N. El-Masry, and S. Bedair, J. Electron. Mater. **44**, 4161 (2015).
[13]F. C.-P. Massabuau, M. J. Davies, F. Oehler, S. K. Pamenter, E. J. Thrush, M. J. Kappers, A. Kovács, T. Williams, M. A. Hopkins, C. J. Humphreys, P. Dawson, R. E. Dunin-Borkowski, J. Etheridge, D. W. E. Allsopp, and R. A. Oliver, Appl. Phys. Lett. **105**, 112110 (2014).
[14]C. De Santi, M. Meneghini, M. La Grassa, B. Galler, R. Zeisel, M. Goano, S. Dominici, M. Mandurrino, F. Bertazzi, D. Robidas, G. Meneghesso, and E. Zanoni, J. Appl. Phys. **119**, 094501 (2016).
[15]A. Alkauskas, C. E. Dreyer, J. L. Lyons, and C. G. Van de Walle, Phys. Rev. B **93**, 201304 (2016).
[16]C. Rauch, I. Makkonen, and F. Tuomisto, Phys. Rev. B **84**, 125201 (2011).
[17]A. Uedono, S. Ishibashi, T. Watanabe, X. Q. Wang, S. T. Liu, G. Chen, L. W. Sang, M. Sumiya, and B. Shen, J. Appl. Phys. **112**, 014507 (2012).
[18]A. Uedono, K. Kurihara, N. Yoshihara, S. Nagao, and S. Ishibashi, Appl. Phys. Lett. **8**, 051002 (2015).
[19]F. Tuomisto and I. Makkonen, Rev. Mod. Phys. **85**, 1583 (2013).
[20]J. Biersack and L. Haggmark, Nucl. Instrum. Methods **174**, 257 (1980).
[21]F. Linez, M. Ritt, C. Rauch, L. Kilanski, S. Choi, J. Räisänen, J. S. Speck, and F. Tuomisto, J. Phys.: Conf. Ser. **505**, 012012 (2014).
[22]J. P. Perdew and A. Zunger, Phys. Rev. B **23**, 5048 (1981).
[23]G. Kresse and J. Furthmüller, Phys. Rev. B **54**, 11169 (1996); Comput. Mater. Sci. **6**, 15 (1996).
[24]G. Kresse and D. Joubert, Phys. Rev. B **59**, 1758 (1999).
[25]E. Boroński and R. M. Nieminen, Phys. Rev. B **34**, 3820 (1986).
[26]I. Makkonen, M. Hakala, and M. Puska, J. Phys. Chem. Solids **66**, 1128 (2005); Phys. Rev. B **73**, 035103 (2006).
[27]J. Oila, V. Ranki, J. Kivioja, K. Saarinen, P. Hautojärvi, J. Likonen, J. M. Baranowski, K. Pakula, T. Suski, M. Leszczynski, and I. Grzegory, Phys. Rev. B **63**, 045205 (2001).
[28]F. Tuomisto, V. Norrman, and I. Makkonen, J. Phys.: Conf. Ser. **505**, 012042 (2014).
[29]S. Ishibashi and A. Uedono, J. Phys.: Conf. Ser. **674**, 012020 (2016).
[30]C. E. Dreyer, A. Alkauskas, J. L. Lyons, J. S. Speck, and C. G. Van de Walle, Appl. Phys. Lett. **108**, 141101 (2016).
[31]G. Miceli and A. Pasquarello, Microelectron. Eng. **147**, 51 (2015).
[32]A. Janotti, J. L. Lyons, and C. G. Van de Walle, Phys. Status Solidi A **209**, 65 (2012).
[33]F. Tuomisto, A. Pelli, K. M. Yu, W. Walukiewicz, and W. J. Schaff, Phys. Rev. B **75**, 193201 (2007).
[34]S. Kilpeläinen, F. Tuomisto, J. Slotte, J. L. Hansen, and A. N. Larsen, Phys. Rev. B **83**, 094115 (2011).
[35]P. Dawson, S. Schulz, R. A. Oliver, M. J. Kappers, and C. J. Humphreys, J. Appl. Phys. **119**, 181505 (2016).
[36]X. Shang, M. D. Luca, G. Pettinari, G. Bisognin, L. Amidani, E. Fonda, F. Boscherini, M. Berti, and G. Ciatto, J. Phys. D: Appl. Phys. **47**, 415301 (2014).
[37]V. Kachkanov, K. P. O'Donnell, R. W. Martin, J. F. W. Mosselmans, and S. Pereira, Appl. Phys. Lett. **89**, 101908 (2006).
[38]M. J. Galtrey, R. A. Oliver, M. J. Kappers, C. J. Humphreys, D. J. Stokes, P. H. Clifton, and A. Cerezo, Appl. Phys. Lett. **90**, 061903 (2007).
[39]J. A. Chan, J. Z. Liu, and A. Zunger, Phys. Rev. B **82**, 045112 (2010).